Message in Message for Improved LoRaWAN Capacity

Takwa Attia, Martin Heusse, Andrzej Duda

Message in Message for Improved LoRaWAN Capacity

Takwa Attia, Martin Heusse, and Andrzej Duda
Univ. Grenoble Alpes, CNRS, Grenoble INP, LIG, 38000 Grenoble, France
Email: {takwa.attia@univ-grenoble-alpes.fr, martin.heusse@imag.fr, andrzej.duda@imag.fr}

***Abstract*—The Aloha-like access method is a major limiting factor in LoRaWAN networks, with only 18% of channel utilization at best. It also causes high packet losses when node deployment becomes more massive.**

In this paper, we propose a technique to enhance the reception process of the LoRaWAN gateways, so that channel utilization can reach values up to 35% in a single LoRaWAN cell.

We investigate the benefits of concurrent and preemptive reception at the gateways: the capture effect allows to receive a frame even if it collides with a later frame, whereas Message in Message (MIM) reception allows the gateway to drop the current reception and switch to a new more powerful frame. An implementation in the NS-3 simulator allows us to assess the gains of this approach through extensive simulations.

***Index Terms*—LoRa, LoRaWAN, Packet Delivery Rate, capture effect, Message in Message**

I. Introduction

LoRa is a low-power long-range technology for the Internet of Things (IoT) [1]. It uses the CHIRP Spread Spectrum (CSS) modulation at the physical layer and a channel access method called LoRaWAN [2]. LoRaWAN defines three types of devices, namely *Class A*, *B*, and *C*. *Class A* devices use pure unslotted ALOHA protocol for the uplink: a device can send a packet at any instant on a chosen radio channel provided its duty cycle follows the frequency band regulations. After sending a packet, a device listens to a response from the gateway during two downlink receive windows. *Class A* results in lowest energy consumption, so we only consider this class in the paper.

The advantage of unslotted ALOHA is its simplicity, but its theoretical performance is low—the channel utilization for ALOHA with fixed packet sizes is around 18%, the result coming from consideration that both frames overlapping in time are lost. When the number of devices increases, unslotted ALOHA results a high level of packet losses [3].

The *capture effect* [4]–[9] increases the theoretical channel utilization because in fact not all colliding frames are lost: the gateway can correctly decode a frame received with higher power when two or more transmissions overlap. The capture effect results in the increased Packet Delivery Probability (*PDR*) and channel utilization. Haxhibeqiri et al. [10] used a simulation model based on the measurements of the interference behavior between two devices with a duty cycle of 1% to show that when their number increases to 1000 per gateway, the loss rate only increases to 32% (multiple channels, multiple SFs, and a payload size of 20 bytes). However, this level of the loss rate should be considered as low compared to 90% in pure unslotted ALOHA for the same load and it results from taking into account the capture effect giving the channel utilization of around 23%.

Message in Message (MIM) further improves the ratio of successful transmissions in case of collisions. In this mechanism not implemented in current LoRaWAN gateways, the receiver may switch to receiving a new stronger frame during the reception of another frame. When the receiver locks on a frame by receiving its preamble and a frame arrives with stronger power, it is beneficial to switch to the stronger frame that has higher probability of correct decoding. Several authors successfully applied MIM to 802.11 or 802.15.4 wireless LANs and showed its benefit of improving transmission reliability [7], [11]–[14].

In this paper, we explore MIM for LoRaWAN and evaluate the extent of improvement it can bring to its capacity. We develop an analytical model for channel utilization in LoRaWAN under multiple concurrent frames and validate its predictions with detailed simulations in NS-3.

Our performance analysis shows the improved channel utilization up to 35% in the scenario of a single LoRaWAN cell, which represents a considerable improvement with respect to the channel utilization of 23% for LoRaWAN with capture effect. Moreover, multiple gateways in a cell can significantly improve capacity with the channel utilization reaching over 40% with two gateways and 60% with four gateways.

In the rest of the paper, we recall the basic principles of LoRaWAN in Section II. Section III discusses the capture effect and introduces MIM. Section IV presents an analytical model of a LoRaWAN cell. We then present the implementation of MIM in NS-3 and report on the evaluation based on simulations in Section V. Section VI discusses previous work and Section VII concludes the paper.

II. LoRa Basics

The physical layer of LoRa defines several parameters [15]:
Bandwidth (*BW*): it is the width of the frequency band occupied by the transmission symbols, or CHIRPs. We can configure the bandwidth between 7.8 kHz and 500 kHz. Larger bandwidth allows for a higher data rate, but results in lower sensitivity.
Spreading Factor (*SF*) characterizes the number of bits carried by a CHIRP: *SF* bits are mapped to one of 2^{SF} possible frequency shifts. *SF* varies between 6 (7 in practice) and

Table I: LoRa parameters for *BW* of 125 kHz.

SF	SNR limit q_j	Airtime τ_j	Data rate DR*j*	PL_{max}
7	-7.5 dB	102.7 ms	DR5: 5469 b/s	230 B
8	-10 dB	184.8 ms	DR4: 3125 b/s	230 B
9	-12.5 dB	328.7 ms	DR3: 1758 b/s	123 B
10	-15 dB	616.5 ms	DR2: 977 b/s	59 B
11	-17.5 dB	1315 ms	DR1: 537 b/s	59 B
12	-20 dB	2466 ms	DR0: 293 b/s	59 B

Figure 1: LoRa frame structure.

12 with *SF12* resulting in the best sensitivity and range, at the cost of achieving the lowest data rate and worst energy consumption. Decreasing the *SF* by 1 unit roughly doubles the transmission rate and divides by 2 the transmission duration as well as energy consumption.

Coding Rate (*CR*): it corresponds to the rate of Forward Error Correction (FEC) applied to improve packet error rate in presence of noise and interference. A lower coding rate results in better robustness, but increases the transmission time and energy consumption. The possible values are: 4/5, 4/6, 4/7, and 4/8.

Transmission Power (*P*): LoRaWAN defines the following values of P for the EU 863-870 MHz band: 2 dBm, 4 dBm, 6 dBm, 8 dBm, 12 dBm, and 14 dBm.

Table I presents the main performance parameters: *SF*, *SNR* limit, the airtime for the maximum payload length (PL_{max}), and data rate.

To understand the capture effect, we need to consider the structure of a LoRa frame at the PHY layer. It starts with a preamble followed by the explicit PHDR header (protected by PHDR_CRC). The frame contains the payload (LoRaWAN MAC frame) protected by the payload CRC [15] (see Figure 1). In explicit mode used in uplink frames, the explicit header contains the information about the payload: its length, *CR*, and the information whether CRC is used or not. The preamble length n_{pr} is programmable from 6 to 65535 symbols (by default, 8 symbols). The LoRa modem adds 4.25 symbols representing the synchronization word. The preamble duration τ_{pr} is defined as [16]:

$$\tau_{\text{pr}} = (n_{\text{pr}} + 4.25) * T_s$$

where T_s is the LoRa symbol duration:

$$T_s = \frac{2^{SF}}{BW}.$$

τ_j, the total frame duration (airtime) at rate DR*j* is the sum of τ_{pr} and the payload duration τ_{pa}:

$$\tau_j = \tau_{\text{pr}} + \tau_{\text{pa}}$$

where

$$\tau_{\text{pa}} = n_{\text{pa}} * T_{sym}$$

and n_{pa} is defined as :

$$n_{\text{pa}} = 8+ \max(\text{ceil}(\frac{8PL - 4SF + 28 + 16 - 20H}{4(SF - 2DE)})(CR + 4), 0),$$

where *PL* is the number of payload bytes, $H = 0$ when the header is enabled and $H = 1$ when there is no header, and $DE = 1$ means low data rate optimization enabled, or disabled ($DE = 0$).

III. Capture Effect and MIM

In wireless random access networks, simultaneous packet receptions are potentially prone to packet collisions resulting in either packet corruption, loss, or successful decoding. Depending on the corresponding reception power, the arrival time of the concurrent packets, and the receiver hardware capabilities, one packet can be correctly received and survive a collision. Therefore, the reception scheme defining how the receiver handles packet concurrency is the fundamental feature that directly impacts the network performance and its capacity.

Moreover, modern wireless radio receivers include more advanced mechanisms to tackle overlapping packet transmissions: for instance, they can foster the *capture effect* or can implement some form of *Message in Message* reception. These functionalities allow receiving at least a fraction of the colliding packets instead of losing them all.

We define the following terms useful to explain different reception schemes:

- **Received Signal Strength Indicator (*RSSI*)**, an indicator of received signal power.
- **Signal to Interference plus Noise Ratio (*SINR*)**, the difference in dB between the involved signal reception powers.
- **Capture Threshold**: the capture is possible if *SINR* is above this threshold.
- **Capture Window**: the capture is possible if the concurrent signal arrives during the time interval.

From the received signal power point of view, we will distinguish between two possible key scenarios:

- **Stronger First:** the stronger packet arrives before the weaker one.
- **Stronger Last:** the stronger comes after the weaker one.

We define five possible reception schemes:

Collision. Both simultaneously transmitted packets are lost.

Simple capture. The receiver can capture one frame according to the Stronger First scenario if it satisfies the Capture Threshold. The receiver locks on the stronger frame and keeps its reception even if any weaker frame arrives later. However, the receiver is unable to capture the stronger frame in the Stronger Last scenario: even if it arrives after the weaker one, both are lost regardless of the difference in power.

Advanced capture. It corresponds to the situation in which the reception is correct if the interfering frame arrives after the preamble of the transmitted frame with the same *RSSI* (*SINR* ≥ 0 dB) [10].

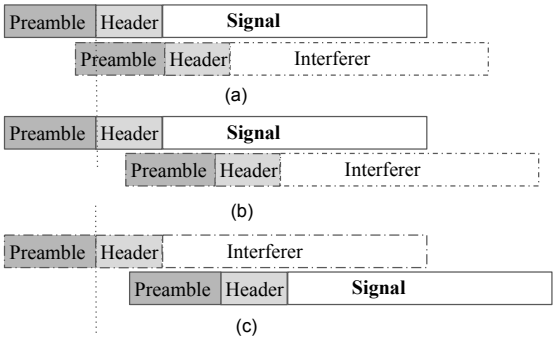

Figure 2: Capture scenarios at the receiver: a) **Simple capture** if *SINR* $\geq$ 6dB, b) **Advanced capture** if an interferer arrives after the preamble duration and *SINR* $\geq$ 0 dB, c) **Physical capture** when the receiver switches to the incoming stronger frame if it arrives during the header of the interferer and *SINR* $\geq$ 6dB. The continuous line denotes the correctly received frame.

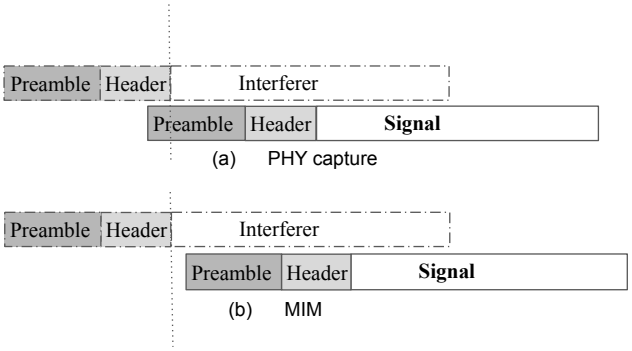

Figure 3: **Physical capture** versus **MIM**: a) **Physical capture**: the receiver switches to the incoming stronger frame if it arrives during the header of the interferer and *SINR* $\geq$ 6 dB, b) **MIM**: the receiver switches to the incoming stronger frame even though it arrives after the header of an interferer and *SINR* $\geq$ 8 dB. Continuous line denotes the correctly received frame.

Physical capture. The receiver can capture the stronger frame in the Stronger Last scenario only if it satisfies the Capture Threshold and it arrives during the Capture Window corresponding in 802.11 to the frame preamble [7], [11]. In this case, the receiver drops the reception of the ongoing weaker frame and locks on the stronger one.

Message in Message (MIM). This scheme enables the receiver to switch from the ongoing reception of a weaker frame to the newly arriving stronger frame as long as the latter frame dominates the former one by a sufficient margin θ_{MR} [6], [7], [11]. The receiver thus drops the ongoing reception and locks on the new frame. The signal of the weaker frame becomes interference to the ongoing reception. For a LoRaWAN gateway, MIM reception would be possible by keeping on monitoring the channel for a preamble even if the reception is active at a given *SF* just like the gateways keep on looking for frames transmitted at other *SFs*. To filter out the signal from the ongoing reception, its received power plus a margin defines the threshold power for the new incoming transmission to switch to. Formally, the receiver switches to another frame if the following condition is satisfied:

$$P_i > \theta_{\text{MR}} = \delta_{\text{MR}} P_l, \tag{1}$$

where P_i is the reception power of the new incoming frame, δ_{MR} is the capture threshold, and P_l is the power of the packet the receives is locked on.

A. Capture Effect and MIM in LoRaWAN

LoRa is a wireless network subject to a high collision rate due to its ALOHA access method that exacerbates the collision issue because there is no predefined scheduling nor the listening before talk mechanism.

The difference of LoRa with the capture schemes defined for 802.11 or 802.15.4 is that we need to consider the arrival instant of the second frame with respect to the preamble and the PHY header (see Figure 2). We can observe **Simple capture** in Figure 2a, the **Advanced capture** in Figure 2b, and **Physical capture** in Figure 2c.

Figure 3 explains the difference between the **Physical capture** and **MIM**. The **Physical capture** enables the receiver to switch to the stronger frame when it arrives during the header and *SINR* $\geq$ 6 dB while in MIM, the receiver switches to the incoming stronger frame even though it arrives after the header of an interferer and *SINR* $\geq$ 8 dB. We use the value of 8 dB for the power margin triggering MIM reception, the same value as needed for MIM in 802.11 [9].

IV. Analytical model for channel utilization with capture

We present below the analytical model for channel utilization in LoRaWAN assuming multiple concurrent frames. It is an extension of our previous work on modeling LoRaWAN capacity [3] under the assumption of a realistic Rayleigh channel [17]. Then, we derive the expression for *PDR* that takes into account the capture effect with several overlapping frames and gives us channel utilization U as a function of *PDR* and offered load v in Erlang:

$$U = PDR \times v.$$

We assume that node $i, i \in \{1...K\}$ generates a packet of length PL_i with airtime τ_i according to a Poisson process of intensity λ_t (the application period between sending a packet is $1/\lambda_t$ for all nodes). Even if the application period is usually constant, the packet generation process in a network with a large number of non-synchronized nodes converges to a Poisson process.

Table I summarizes the notation.

A. Successful reception probability under unslotted ALOHA

We consider all nodes operating with a given data rate DR*j* and denote by $v_j = k_j \, \tau_j \, \lambda_t$ their offered load in Erlang. The

Table II: Notation

Packet generation intensity	λ_t
Number of nodes using data rate DRj	k_j
Number of nodes	K
Frame transmission duration at data rate DRj	τ_j
Offered traffic (in Erlang) at DRj	v_j
Overall offered traffic (in Erlang)	v
Channel utilization	U
Average channel gain at distance d	$g(d)$
SNR threshold for DRj	q_j
Power gap for successful capture (typically 0 dB)	ξ
Transmission power	P
Received power at DR_i	P_i^{rx}
In-band noise power	$\mathcal{N}$

probability of successful reception under unslotted ALOHA is subject to two conditions:

1) no other frame occupies the channel at the moment the transmission of interest starts, which happens with probability e^{-v_j} and no other transmission starts while it is ongoing (which happens with the same probability e^{-v_j}). So, the probability of a collision-free transmission is just:

$$e^{-2v_j}$$

2) the signal power at the gateway is above the demodulation floor. This condition is met when the Rayleigh channel gain is above

$$g_{\text{t}} = \frac{\mathcal{N}\, q_j}{P\, g(d)},$$

which happens with probability $e^{-g_{\text{t}}}$, where $\mathcal{N}$ is the constant thermal noise, q_j is the SNR threshold for DRj, P transmission power, and $g(d)$ is the average channel gain at distance d [3]. For instance, $\mathcal{N} = -123\,\text{dBm}$ ($-174\,\text{dBm}$ per Hz) for a 125 kHz-wide frequency band.

B. Successful reception under unslotted ALOHA with multiple overlapping frames

There are two conditions for the successful reception of a packet under this model:

- if a frame occupies the channel when the frame of interest arrives, then we consider that this latter is lost: if the receiver was not locked on the previous frame, synchronization would be possible. So, successful frame reception requires the absence of any transmission during time τ_j before the frame transmission, which happens with probability:
$$e^{-v_j},$$
- once the reception of the frame of interest starts, it will succeed if the sum of the powers of the interfering frames does not exceed ξ.

We derive $PDR_{\text{D}}^{\Sigma}(N)$, the reception probability of a frame when competing against N other simultaneous transmissions as follows, where $f_\Sigma(N,x)$ is the probability density function of the sum of powers from N transmissions:

$$\begin{aligned}
PDR_{\text{D}}^{\Sigma}(N) &= \int_0^\infty f_\Sigma(N,x) \int_{\max(g_{\text{t}},\xi x)}^\infty e^{-y}\,dy\,dx \\
&= \int_0^{\frac{g_{\text{t}}}{\xi}} f_\Sigma(N,x) \int_{g_{\text{t}}}^\infty e^{-y}\,dy\,dx \\
&\quad + \int_{\frac{g_{\text{t}}}{\xi}}^\infty f_\Sigma(N,x) \int_{\xi x}^\infty e^{-y}\,dy\,dx \\
&= \frac{1}{(N-1)!}\Bigg(e^{-g_{\text{t}}} \int_0^{\frac{g_{\text{t}}}{\xi}} e^{-x} x^{N-1}\,dx \\
&\quad + \int_{\frac{g_{\text{t}}}{\xi}}^\infty x^{N-1} e^{-(\xi+1)x}\,dx\Bigg) \\
&= \frac{1}{(N-1)!}\Bigg(e^{-g_{\text{t}}}\gamma(N,\frac{g_{\text{t}}}{\xi}) \\
&+ \frac{1}{(\xi+1)^{N-1}} \int_{\frac{g_{\text{t}}}{\xi}}^\infty [(\xi+1)x]^{N-1} e^{-(\xi+1)x} dx\Bigg) \\
&= \frac{1}{(N-1)!}\Bigg(e^{-g_{\text{t}}}\gamma(N,\frac{g_{\text{t}}}{\xi}) \\
&\quad + \frac{1}{(\xi+1)^{N}} \int_{\frac{(\xi+1)g_{\text{t}}}{\xi}}^\infty u^{N-1} e^{-u}\,du\Bigg) \\
&= \frac{1}{(N-1)!}\Bigg(e^{-g_{\text{t}}}\gamma\left(N,\frac{g_{\text{t}}}{\xi}\right) \\
&\quad + \frac{1}{(\xi+1)^{N}}\Gamma\left(N,\frac{(\xi+1)g_{\text{t}}}{\xi}\right)\Bigg),
\end{aligned}$$

where $\gamma(N,x)$ is the lower incomplete gamma function and $\Gamma(N,x)$ is the upper incomplete gamma function.

Combining the probability of success against N other frames with the probability of overlapping this number of frames yields the average *PDR*. We assume that the packet arrival process is Poisson, so the probability that a frame intersects N other frames is:

$$\Pr[N] = \frac{(v_j)^N}{N!} e^{-v_j}.$$

Successful reception is also conditioned by an empty channel when the reception of the frame of interest starts, which happens with probability e^{-v_j}. Thus:

$$\begin{aligned}
PDR_{\text{D,T}}^{\Sigma} &= e^{-v_j}\, e^{-v_j}\left(e^{-g_{\text{t}}} + \sum_{N=1}^{\infty} \frac{(v_j)^N}{N!} PDR_{\text{D}}^{\Sigma}(N)\right) \quad (2) \\
&= e^{-2v_j}\left(e^{-g_{\text{t}}} + \sum_{N=1}^{\infty} \frac{(v_j)^N}{N!} PDR_{\text{D}}^{\Sigma}(N)\right). \quad (3)
\end{aligned}$$

From this expression, we can obtain utilization U.

V. Evaluation with NS-3 Simulations

The goal of the evaluation is to investigate the impact of different reception schemes on the single-channel capacity with several scenarios and configurations. We opted for simulations because experimental validation would require a network with a large number of devices to observe collisions. Nevertheless,

we carefully validated the NS-3 simulator to obtain meaningful results.

We have modified and extended the NS-3 LoRa module developed by Magrin et al. [18] with the capture schemes and MIM.[1] The module implements several features: Adaptive Data Rate (ADR), downlink traffic, multiple reception paths at the gateway, Duty Cycle (DC) limitation, co-spreading interference matrix, and retransmissions. Since our study focuses on the reception schemes at the gateway, the features are disabled except for DC limited to 1%.

A. LoRa Channnel Model for NS-3

We wanted our simulations as realistic as possible so we used an adequate channel model closely representing the real LoRa channel. A packet transmission is subject to both large scale and a small scale fading. For the large scale, we adopted the lognormal path loss as it is the most used for attenuation in suburban cities, also used by Magrin et al. [18], defined as:

$$L^{dB}(d) = L(d_0) + 10 * \eta * \log_{10}(\frac{d}{d_0}),$$

where $L(d_0)$ is the reference path loss based on measurements at distance d_0, η is the path loss or propagation exponent that determines at which rate the path loss increases with distance [19]. More specifically, L in suburban environments is given as:

$$\begin{aligned} L^{dB}(d) = 40(1 - 4 * 10^{-3} * h)\log_{10}(d) \\ -18\log_{10}(h) + 21\log_{10}(fr) + 80, \end{aligned}$$

where $h \in [0, 50]$ is the antenna elevation, *fr* is the frequency in MHz. For *fr* = 868 MHz and $h = 15$ m, we obtain:

$$L^{dB}(d) = 120.5 + 10 * 3.76 * \log_{10}(d).$$

In our previous work [3], [17], we showed through experimental validation on a testbed that the LoRa channel behaves like a Rayleigh fading channel. NS-3 includes the Nakagami-m model, a more generalized formula than Rayleigh: for $m = 1$, it corresponds to Rayleigh. The Nakagami probability density function is as follows:

$$f(x; m, w) = \frac{2m^m}{\Gamma(m)w^m} x^{2m-1} e^{-\frac{m}{w} * x^2},$$

where m is the fading depth parameter and w the average received power. For $m = 1$, the distribution is Rayleigh:

$$f_1(x; w) = \frac{x}{w^2} e^{-\frac{x^2}{2w^2}},$$

and the received power follows an exponential distribution.

B. Capture Schemes in LoRaWAN

Implementing the most relevant capture schemes that mimic the real physical behavior of the gateway is challenging yet fundamental for obtaining accurate simulation results, notably with LoRaWAN in which the capture impact is significant in increasing the throughput of the network. Below, we present the implementation of the several reception schemes described above in the NS-3 simulator.

We assume that a Signal (or frame) of Interest (SoI) may face multiple colliding packets depending on the network load. We use the following notation: I^i is the set of interferers transmitting at rate DRi that collide with SoI. I^i_k is the k^{th} interferer, $k \in \{1..n_I\}$, where n_I is the number of frames colliding with SoI. Its reception power is $P^{\text{rx}}_{I^i_k}$ and that of SoI, $P^{\text{rx}}_{\text{SoI}}$.

LoRaWAN Simple capture. The simulator computes *SINR* between $P^{\text{rx}}_{\text{SoI}}$ and the received power of the strongest interferer denoted by k^*, $P^{\text{rx}}_{k^*}$ as:

$$\textit{SINR} = \frac{P^{\text{rx}}_{\text{SoI}}}{P^{\text{rx}}_{k^*}}, \text{ where } P^{\text{rx}}_{k^*} = \max_k P^{\text{rx}}_k.$$

If $\textit{SINR} \geq 6dB$ [20], then the SoI packet survives and can be decoded. The scheme is independent of the arrival timing of the concurrent packets and SoI.

LoRaWAN Advanced capture. In this scheme, the required power difference between the interferer and SoI goes from 6 dB to 0 dB if the interferer arrives after the end of the SoI preamble. Let $I^i_1 = \{I^i_{1,1}..I^i_{1,k}...I^i_{1,n_{1,I}}\}$ denote the subset of interferers that arrive before the SoI preamble and $I^i_2 = \{I^i_{2,1}..I^i_{2,k}...I^i_{2,n_{2,I}}\}$ those arriving after. k^*_1 and k^*_2 are the indices of the strongest interferer of I^i_1 and I^i_2, respectively. We define $\textit{SINR}_1$ and $\textit{SINR}_2$ as:

$$\textit{SINR}_1 = \frac{P^{\text{rx}}_{\text{SoI}}}{P^{\text{rx}}_{k^*_1}}, \text{ where } P^{\text{rx}}_{k^*_1} = \max_{k_1} P^{\text{rx}}_{k_1}.$$

$$\textit{SINR}_2 = \frac{P^{\text{rx}}_{\text{SoI}}}{P^{\text{rx}}_{k^*_2}}, \text{ where } P^{\text{rx}}_{k^*_2} = \max_{k_2} P^{\text{rx}}_{k_2}.$$

SoI survives collisions only and only if $\textit{SINR}_1 \geq 6$ dB and $\textit{SINR}_2 \geq 0$ dB.

LoRaWAN Physical capture. In the physical capture, the receiver can switch to an incoming packet depending on the arrival time and reception power of both packets. Let t_1 and t_2 denote the respective arrival instants of the Locked-on-Packet (LoP) and the New-incoming-Packet (NiP), P^{rx}_1 and P^{rx}_2 are the received powers of LoP and NiP, respectively, $\tau_{\text{pr},1}$ and $\tau_{\text{hd},1}$ are the preamble and header durations of LoP, respectively. We define *SINR* as:

$$\textit{SINR} = \frac{P^{\text{rx}}_2}{P^{\text{rx}}_1}.$$

The physical capture of NiP happens only and only if $\textit{SINR} \geq 6$ dB and $t_1 + \tau_{\text{pr},1} < t_2 < t_1 + \tau_{\text{hd},1}$.

LoRaWAN MIM. Unlike physical capture, MIM has the advantage of being independent of any capture window, i.e., the arrival time of NiP with respect to LoP. It only depends on the capture threshold (*SINR*) that should be higher than 8 dB. Therefore, the receiver can switch to NiP if $\textit{SINR} \geq 8$ dB, where:

$$\textit{SINR} = \frac{P^{\text{rx}}_2}{P^{\text{rx}}_1},$$

with P^{rx}_1 and P^{rx}_2 the reception powers of LoP and NiP, respectively.

[1] https://gricad-gitlab.univ-grenoble-alpes.fr/attiata/lorawan-ns3

Table III: Simulation parameters

Parameter	Value(s)[unit]
Number of devices	0 to 10000
Cell radius R	2,500, 7,500 m
Packet length	59 B
Transmission power P	14 dBm
Spreading Factor *SF*	12
Bandwidth	250 KHz
Frequency bands	868 MHz
Duty cycle	1%
SNR threshold for DR*j*	Table I
Available reception paths	8
Enabled reception path	1
Path loss	Log Normal
Fading	Rayleigh fading
ADR	disabled
Retransmissions	disabled

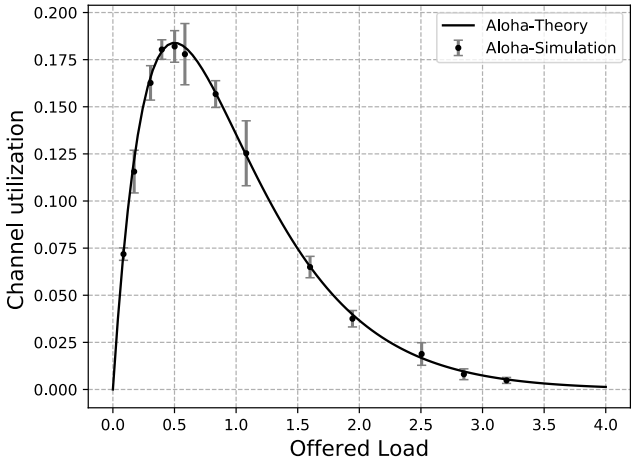

Figure 4: Comparison of the theoretical ALOHA utilization with simulation.

In MIM and the physical capture scheme, the receiver after locking on NiP, will perform advanced capture of NiP in the presence of other colliding packets. If it satisfies the required condition for successful reception with advanced capture, the receiver can correctly decode the packet. The fact that the receiver is locked on NiP that now becomes SoI, does not make it immune to collisions from other packets that can potentially arrive later. Only its high received power compared to other packets can guarantee its successful reception.

C. Simulation Setup

In the evaluation, we consider two scenarios: a) uniformly distributed nodes in a given range R and b) all nodes in the same place at a given distance R. In both scenarios, *SF* is the same for all nodes because we analyze the performance of a single channel characterized by the couple (frequency, *SF*). The first scenario corresponds to the conditions favorable to capture effect—nodes face different channel attenuation resulting in a difference in their received powers at the gateway. The second scenario is the worst case for capture effect—all nodes are subject to the same attenuation so their packets have similar reception powers.

Devices periodically generate a packet according to the configured application period respecting the duty cycle. All devices generate the same amount of traffic. We only consider uplink traffic with disabled ADR and retransmissions. Table III summarizes all simulation parameters.

D. Simulator Validation

We start with the validation of the simulator in a scenario with a given number of nodes uniformly distributed in a cell of radius $R = 2,500$ m around a single gateway using *SF12* and P of 14 dBm under path loss attenuation without capture effect. Figure 4 presents the comparison of the theoretical ALOHA utilization with simulation results along with 95% confidence intervals showing good agreement with the theory.

E. Simulation Results for Different Reception Schemes

We have evaluated the reception schemes in a cell with the ranges $R = 2,500$ m and $R = 7,500$ m, using *SF12* and transmission power P of 14 dBm under path loss and Rayleigh fading. Figures 5 and 6 show the utilization as a function of offered load in Erlang for all the reception schemes. We can observe that MIM outperforms all other reception schemes. However, the difference between MIM and other schemes depends on the node distribution and the distance to the gateway. For instance, in Figures 5a and 6a under MIM, the gateway can receive more packets than with the other reception schemes provided the fundamental condition is satisfied: the gap in powers between concurrent packets should be above 8 dB. As we may expect, at the distance of 7,500 m from the gateway, nodes suffer from important attenuation compared to the distance of 2,500 m.

For the second scenario of nodes at the same place presented in Figures 5b and 6b, all capture schemes exhibit almost the same performance because there is less opportunity to benefit from capture effect. Nevertheless, the advanced capture has better performance than ALOHA because the receiver tolerates capture at 0 dB for all packets that arrive after the SoI preamble. ALOHA drops to 12% of channel utilization and simple capture peaks at 18%.

For high channel load ($v_0 > 2$) corresponding to 5,000 nodes and above up to 21,000 nodes ($v_0 = 7$ in Figure 5a), MIM shows a high and almost stable channel utilization, compared to simple, advanced, and physical capture. The utilization of these schemes begins to drop after load greater than $v_0 = 1$ due to collisions and concurrency.

We can conclude from these results that MIM obtains remarkable performance in usual conditions in which nodes are distributed over some area and it copes with the increased load better than other reception schemes.

Figures 7 and 8 explore a setup with multiple gateways under the MIM scheme and physical capture, respectively: nodes are uniformly distributed in a cell of radius 7,500 and gateways are at the same place, but we assume that the antennas are sufficiently far away from each other to achieve

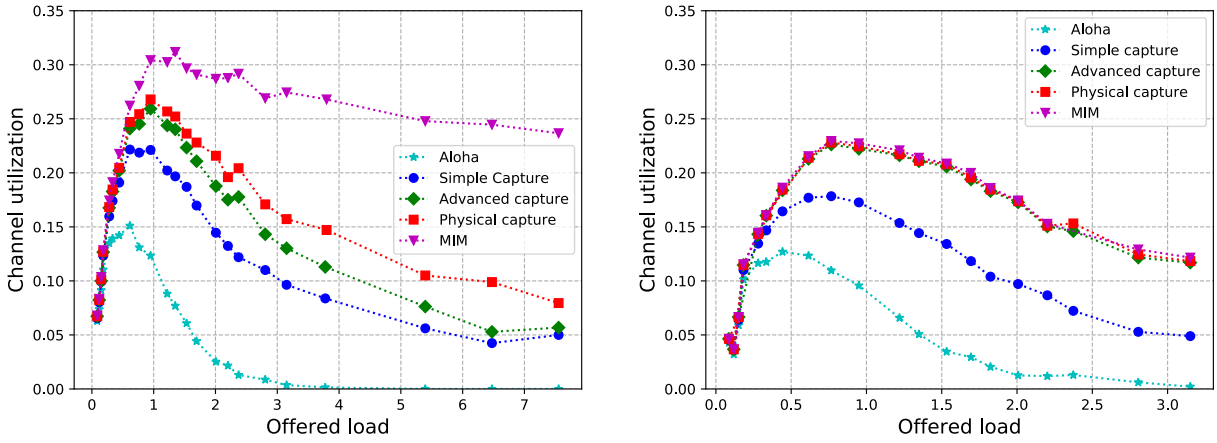

Figure 5: Channel utilization vs. offered load in Erlang for *SF12*, $P = 14$ dBm at 7,500 m: a) uniformly distributed nodes, b) nodes at the same place.

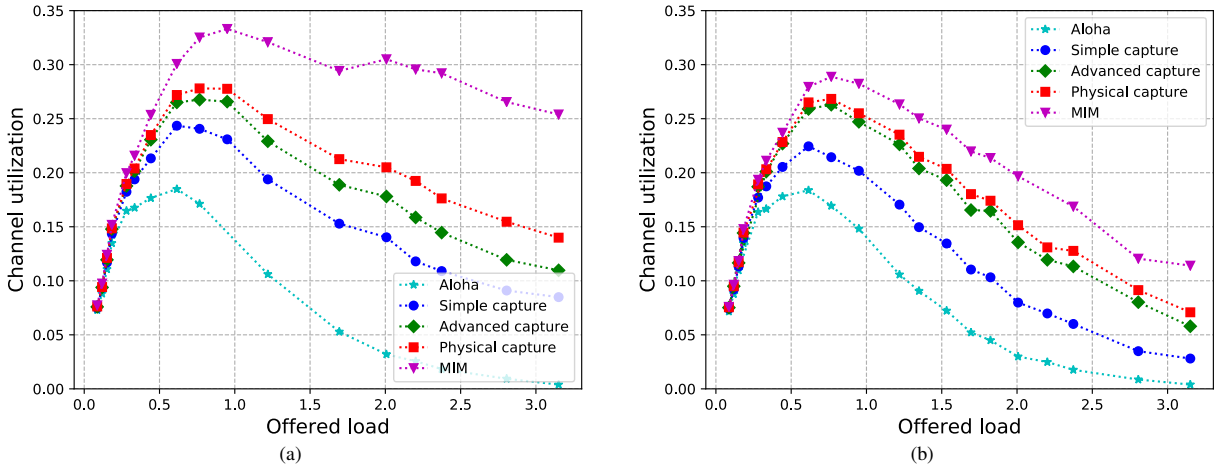

Figure 6: Channel utilization vs. offered load in Erlang for *SF12*, $P = 14$ dBm at 2,500 m: a) uniformly distributed nodes, b) nodes at the same place.

different small-scale fading. We can observe in Figures 7 and 8 that multiple gateways significantly improve the capacity of the cell with the channel utilization reaching over 40% for two gateways and 60% for four gateways in Figure 7 and peaks at 35% for two gateways and at 45% for four gateways in Figure 8. Interestingly, the overall channel utilization for three gateways with MIM outperforms four gateways with physical capture. For high load ($v_0 > 3$), two gateways with MIM outperform four gateways with physical capture, therefore increasing the efficiency and maximizing the capacity of the network.

Figures 9 and 10 present the results of the analytical model detailed in Section IV compared with the simulation results (95% confidence intervals) for a cell with a single gateway. In the simulation, we have adopted the same assumptions as in the analytical model: i) if there is any other frame that arrived before SoI, then we consider the latter lost and ii) the capture of SoI is successful if the power of the signal is equal to the sum of the power of all overlapping frames at DR_i, i.e., $SINR > 0$.

Figure 9 corresponds to the scenario in which nodes are at the same place at distance $R = 2,500$ m and at distance $R = 7,500$ m in Figure 10. The simulation assumes the Rayleigh and path loss channel with all nodes using the same $SF = 12$ and $P = 14$ dBm. The figures also show the results for pure ALOHA for comparison.

We can notice that the simulation results perfectly fit the analytical model for $R = 2,500$ m and are very close to simulation for $R = 7,500$ m. The assumptions of the model are close to the previously presented advanced capture in which $SINR \geq 0$ with packets arriving after the preamble of SoI.

VI. Related work

Many studies examined the Lora capture experimentally and identified many reception schemes. Haxhibeqiri et al. [10] investigated physical capture in LoRa networks. They showed

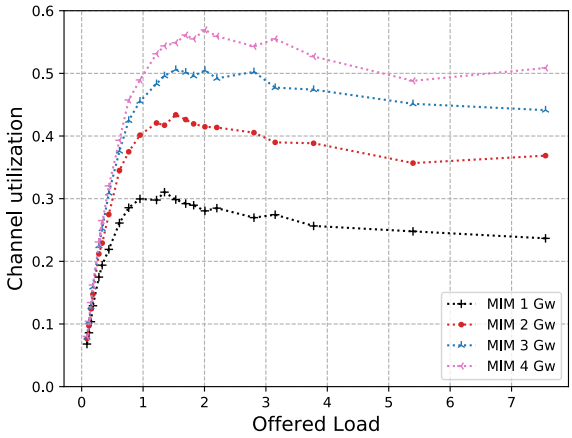

Figure 7: Channel utilization vs. offered load in Erlang for multiple gateways under MIM. Nodes are uniformly distributed in a cell with radius $R = 7,500\,\text{m}$, $SF = 12$, and $P = 14\,\text{dBm}$. Gateways at the same place.

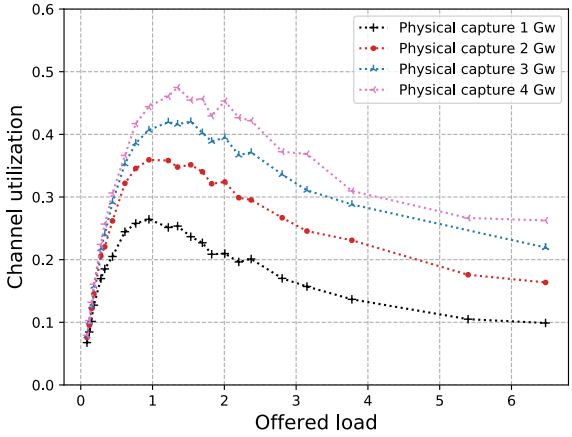

Figure 8: Channel utilization vs. offered load in Erlang for multiple gateways under physical capture. Nodes are uniformly distributed in a cell with radius $R = 7,500\,\text{m}$, $SF = 12$, and $P = 14\,\text{dBm}$. Gateways at the same place.

that the capture effect depends on two main parameters: i) the arrival instant of a transmitted frame (Signal of Interest, SoI) relative to the interfering frame and ii) the Received Signal Strength Indicators (*RSSI*) of the transmitted and interfering frames.

Rahmadhani et al. [21] studied LoRaWAN frame collisions and capture effect through experiments based on the application level side. They focus on the frame loss due to collisions between a weak and a strong frame. They distinguish four cases similar to the results of Haxhibeqiri et al. [10].

Magrin et al. [18] have implemented the capture effect in NS-3 as follows. For every interferer and a packet arriving with the same *SF* during the reception of SoI, they compute related energy and the sum all energy of different interferers to obtain *SINR*. Then, they compare the resulting *SINR* with

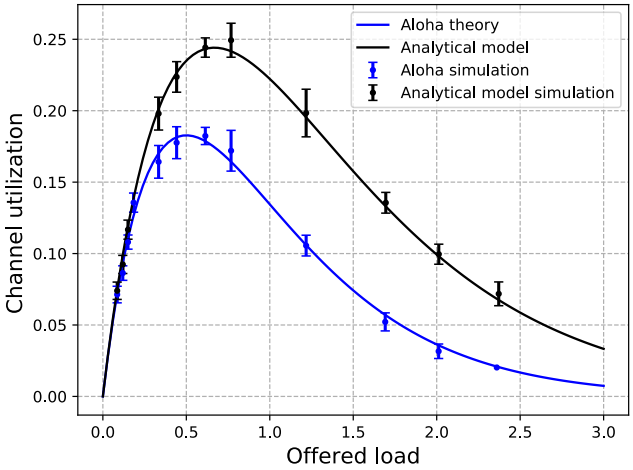

Figure 9: Comparison of the analytical model results with simulation. Channel utilization vs. offered load in Erlang. Nodes at the same place at distance $R = 2,500\,\text{m}$, single gateway.

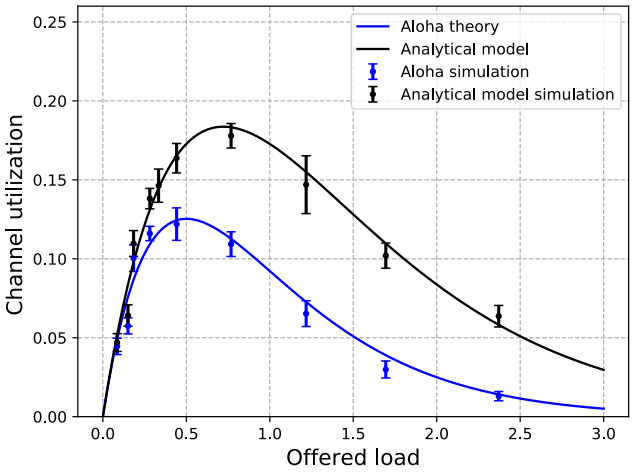

Figure 10: Comparison of the analytical model results with simulation. Channel utilization vs. offered load in Erlang. Nodes at the same place at distance $R = 7,500\,\text{m}$, single gateway.

the value from the collision matrix [20].

This approach is optimistic compared to a realistic operation of LoRa. In fact, if we consider a strong packet that interferes only during a short period with SoI, using this approach, resulting energy could be negligible with respect to total energy of SoI. However, in real world scenarios, this interferer can corrupt SoI, so the packet that should be considered lost is considered as successfully received. Such an approach could have been correct if the frequency band were wider, like in UMTS for instance, where the correction code, channel coding, and equalization techniques at the receiver could reconstruct/regenerate a packet from a correctly received part. However, such operation is not possible with LoRa for which,

when we lose a packet because of a collision or the channel fading, it is lost in totality as we showed in our previous work [17].

Choir [22] leverages the frequency offsets introduced by the imperfect hardware nature of LPWAN to disentangle and decode concurrent colliding transmissions. This technique would allow to decode several packets simultaneously but there is no proof of whether it is applicable in a massive network. For instance, as the number of concurrent transmissions increases, it becomes more challenging to distinguish between the FFT peaks from different transmitters. Moreover, in presence of moving transmitters or scatterers, different propagation paths correspond to different frequency shifts, which makes things even more arduous, as several FFT peaks correspond to the same sender.

VII. Conclusion

In an LPWAN context, we study the potential benefits of MIM, a relatively common reception scheme in WLAN networks. MIM allows a stronger signal to be received even if the receiver is locked on the reception of a weaker frame. MIM is promising for LPWANs because of the ALOHA access method for which collisions are extremely common. Moreover, nodes are naturally spread over a wide area and Rayleigh fading introduces additional variability to the reception power. Consequently, we expect that reception preemption may be frequent even with a significant power margin for triggering the switch.

In this paper, before exploring the benefits of MIM, we have carefully defined the baseline performance, which corresponds to pure ALOHA and ALOHA with capture. We have provided an analytical analysis that corroborates the results obtained with simulation. Based on this foundation, we add MIM when there is a reception margin of 8 dB in favor of the frame arriving later. The performance gains are notable, especially when there is a variability between the channel gains experienced by nodes. Scalability is especially improved when there is a degree of macro-diversity like in the case of multiple gateways. We believe that the results are encouraging enough to justify an effort to implement MIM on real hardware. Actually, MIM reinforces the benefits of having contrasted reception powers between nodes, which calls for considering randomization of transmission powers [23].

Acknowledgments

This work has been partially supported by the French Ministry of Research projects PERSYVAL-Lab under contract ANR-11-LABX-0025-01 and DiNS under contract ANR-19-CE25-0009-01.

References

[1] LoRa™ Alliance, "A Technical Overview of LoRa and LoRaWAN," 2015. [Online]. Available: {https://www.lora-alliance.org/lorawan-white-papers}

[2] N. Sornin *et al.*, "LoRaWAN Specification v1.1," 2017. [Online]. Available: https://lora-alliance.org/resource-hub/lorawantm-specification-v11

[3] M. Heusse, T. Attia, C. Caillouet, F. Rousseau, and A. Duda, "Capacity of a LoRaWAN Cell," in *Proc. ACM MSWiM '20*, 2020, pp. 131–140.

[4] C. Lau and C. Leung, "Capture Models for Mobile Packet Radio Networks," *IEEE Trans. Commun.*, vol. 40, pp. 917–925, 1992.

[5] J. Boer *et al.*, "Wireless LAN with Enhanced Capture Provision," US Patent 5987033, 1999.

[6] C. Ware, J. F. Chicharo, and T. A. Wysocki, "Simulation of Capture Behaviour in IEEE 802.11 Radio Modems," in *Proc. IEEE VTC Fall 2001, Atlantic City, New Jersey, USA*, 2001, pp. 1393–1397.

[7] A. Kochut, A. Vasan, A. U. Shankar, and A. K. Agrawala, "Sniffing Out the Correct Physical Layer Capture Model in 802.11b," in *IEEE ICNP*, Berlin, Germany, 2004, pp. 252–261.

[8] K. Whitehouse, A. Woo, F. Jiang, J. Polastre, and D. Culler, "Exploiting the Capture Effect for Collision Detection and Recovery," in *Proc. the 2nd IEEE Workshop on Embedded Networked Sensors*, 2005, p. 45–52.

[9] J. Lee, W. Kim, S.-J. Lee, D. Jo, J. Ryu, T. Kwon, and Y. Choi, "An Experimental Study on the Capture Effect in 802.11a Networks," in *Proc. of WinTECH '07*, 2007, p. 19–26.

[10] J. Haxhibeqiri, F. V. D. Abeele, I. Moerman, and J. Hoebeke, "LoRa Scalability: A Simulation Model Based on Interference Measurements," *Sensors*, vol. 17, no. 6, p. 1193, 2017.

[11] J. Manweiler, N. Santhapuri, S. Sen, R. R. Choudhury, S. Nelakuditi, and K. Munagala, "Order Matters: Transmission Reordering in Wireless Networks," in *Proc. MOBICOM 2009*, K. G. Shin, Y. Zhang, R. L. Bagrodia, and R. Govindan, Eds., pp. 61–72.

[12] W. Wang, W. K. Leong, and B. Leong, "Potential Pitfalls of the Message in Message Mechanism in Modern 802.11 Networks," in *Proc. WiNTECH '14*, 2014, pp. 41–48.

[13] G. Boudour, M. Heusse, and A. Duda, "An Enhanced Capture Scheme for IEEE 802.15.4 Wireless Sensor Networks," in *Proc. IEEE ICC*. Budapest, Hungary: IEEE, Jun. 2013.

[14] ——, "Improving Performance and Fairness in IEEE 802.15.4 Networks with Capture Effect," in *Proc. IEEE ICC*. Budapest, Hungary: IEEE, Jun. 2013.

[15] Semtech, "SX1272/73 - 860 MHz to 1020 MHz Low Power Long Range Transceiver," 2017. [Online]. Available: https://www.semtech.com/uploads/documents/sx1272.pdf

[16] "Lora modem designer's guide," Semtech Corporation, Tech. Rep., Jul. 2013.

[17] T. Attia, M. Heusse, B. Tourancheau, and A. Duda, "Experimental Characterization of LoRaWAN Link Quality," in *Proc. IEEE GLOBECOM*, 2019, pp. 1–6.

[18] D. Magrin, M. Centenaro, and L. Vangelista, "Performance Evaluation of LoRa Networks in a Smart City Scenario," in *IEEE ICC*, May 2017.

[19] 3GPP, "Radio Frequency (RF) system scenarios,," Jan. 2016.

[20] C. Goursaud and J. M. Gorce, "Dedicated Networks for IoT: PHY/MAC State of the Art and Challenges," *EAI Endorsed Transactions on Internet of Things*, vol. 15, no. 1, 10 2015.

[21] A. Rahmadhani and F. Kuipers, "When LoRaWAN Frames Collide," in *Proc. WiNTECH '18*, 2018, pp. 89–97.

[22] R. Eletreby, D. Zhang, S. Kumar, and O. Yagan, "Empowering Low-Power Wide Area Networks in Urban Settings," in *Proc. SIGCOMM*. ACM, 2017, pp. 309–321.

[23] Y. Birk and Y. Revah, "Increasing Deadline-Constrained Throughput in Multi-Channel ALOHA Networks via Non-Stationary Multiple-Power-Level Transmission Policies," *Wireless Networks*, vol. 11, pp. 523–529, July 2005.